Journal of Molecular Catalysis A: Chemical 308 (2009) 134–141

Contents lists available at ScienceDirect

Journal of Molecular Catalysis A: Chemical

journal homepage: www.elsevier.com/locate/molcata

Dehydration of epiandrosterone over zeolites with different pore structures and acidities

O Zoon Kwon [a], Se Min Park [a], Mee Kyung Song [b], Gon Seo [a,*]

[a] School of Applied Chemical Engineering and the Center for Catalysis Research, Chonnam National University, YongBong 300, Gwangju 500-757, Republic of Korea
[b] Bioinformatics and Molecular Design Research Center, Yonsei Engineering Research Complex, Yonsei University, Seoul 120-749, Republic of Korea

ARTICLE INFO

Article history:
Received 5 December 2008
Received in revised form 26 March 2009
Accepted 30 March 2009
Available online 7 April 2009

Keywords:
Zeolite
Epiandrosterone
Dehydration
Conformation
Adsorption simulation

ABSTRACT

Four kinds of large port zeolites BEA, FAU, LTL and MOR, were used as catalysts in the dehydration of a large molecule, epiandrosterone, to elucidate the effect of their pore structure on its conversion and the selectivity for 5α-androst-2-en-17-one (Δ2-olefin). Silane masking of the zeolite acid sites, measurement of their epiandrosterone uptake, and theoretical calculations to find the energy-minimized conformation in zeolite pores revealed the roles of pore structure and acid sites in the dehydration. LTL and MOR zeolites showed poor conversion and low selectivity for Δ2-olefin because of the close packing in their linear pores. BEA and FAU zeolites with three-dimensionally connected pores exhibited high conversion. Since the supercages of FAU zeolite provided enough space to allow tilted conformation of epiandrosterone with high preference for the formation of Δ2-olefin, FAU zeolites with a sufficient number of acid sites demonstrated both high conversion and selectivity in the dehydration of epiandrosterone.

1. Introduction

Catalysts have been occasionally used in organic reactions of bulky materials [1–6], although their catalytic function is not sufficiently understood and they have typically been considered indispensable materials for the reactions. Little systematic research has been conducted on the interaction between catalysts and large bulky organic reactants. Recently, several papers reported the application of zeolites with specific pore structures to organic synthesis in order to enhance the selectivity for desired products by suppressing the formation of undesired intermediates [1–6]. These trials have been continued because of the difficulty in separating the desired products from their bulky isomers with their very similar structures. They have only a small difference such as the position of double bonds and the coordination direction of substituents. Therefore, a highly selective catalyst for a certain isomer of bulky materials will be very useful for an organic reaction which produces many isomers.

Zeolites have micropores smaller than 1 nm, but they are active for the dehydration reaction of cholesterol [2]. Careful control of the reaction conditions induces a high selectivity for the desired product. Zeolites are also used in the selective photoreduction of olefinic steroids such as testosterone acetate, cholesterone, and androstenedione [3]. Transition metal-loaded zeolites show high selectivity for the hydrogenation of 17β-hydroxy-androst-4-en-3-one due to their pore structures [4]. Selective cyclization of a variety of epoxy polyene terpenes [5] and farnesal [6] induce stereo-controlled products as nanaimoal in zeolite NaY. Although several papers in the literature reported the high feasibility of zeolites as catalysts for bulky organic reactions [2–6], the contribution of their external surface to the selectivity has not been systematically investigated.

The dehydration product of epiandrosterone, 5α-androsten-17-one, has two isomers of 5α-androst-2-en-17-one (Δ2-olefin) and 5α-androst-3-en-17-one (Δ3-olefin) with different positions of their double bonds. However, only Δ2-olefin has been effectively used in the preparation of muscular relaxants [7,8] and aminosteroids [9]. Furthermore, the separation of Δ2-olefin from Δ3-olefin using conventional methods is very difficult, so that the selectivity of catalysts for Δ2-olefin is very important in determining their feasibility.

Several methods for the dehydration of epiandrosterone have been reported, as shown in Scheme 1 [10–16]. The hydroxyl group combined to the 3-C atom of epiandrosterone reacts with *p*-toluenesulfonyl chloride or methane sulfonyl chloride to produce tosylate esters, which can be easily converted to olefins through the elimination reaction over LiBr [10] or base materials such as collidine [11] and lutidine [12]. The so-called Burgess' reagent, the salt of methoxycarbonyl sulfamoyl triethyl ammonium hydroxide, is very active in producing the dehydrated intermediates from epiandrosterone. Δ2-Olefin is selectively obtained by heating the intermediates at 90 °C [13]. The supported acids prepared

* Corresponding author. Tel.: +82 62 530 1876; fax: +82 62 530 1899.
E-mail address: gseo@chonnam.ac.kr (G. Seo).

1381-1169/$ – see front matter © 2009 Elsevier B.V. All rights reserved.
doi:10.1016/j.molcata.2009.03.037

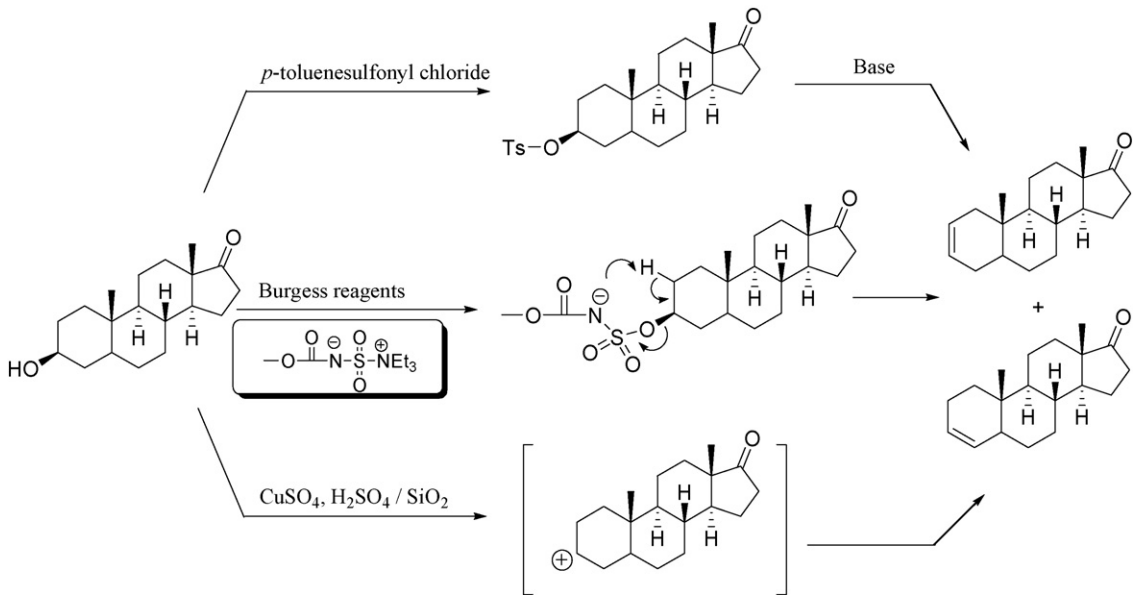

Scheme 1. Several methods for the dehydration of epiandrosterone.

by impregnating sulfuric acid or copper sulfate on silica gel with a diameter of 0.063–0.2 mm were active in the dehydration of epiandrosterone [14–16]. These supported acids produce cationic intermediates and the continuous removal of the produced water by refluxing completes the dehydration reaction.

The homogeneous catalytic reactions using *p*-toluenesulfonic chloride and Burgess' reagent described above achieve high levels of selectivity for Δ2-olefin, but the additional purification of products removing these reagents is essential to obtain Δ2-olefin with sufficient purity to be useful for pharmaceutical production. The equilibrium compositions of Δ2- and Δ3-olefin isomers in the dehydration of epiandrosterone are very close because of the small difference in their Gibbs free energies.

However, the selectivity for Δ2-olefin differs widely according to the catalysts. In our previous work [17], sulfonic acid-incorporated MCM-41 mesoporous materials exhibit an exceptional high selectivity for Δ2-olefin of above 95%, even though the conversion varies from 63 to 99% according to the number of acid sites loaded on them. The tilted orientation of epiandrosterone on their surface reduces the steric hindrance at the adsorption of epiandrosterone on the acid sites and prevents the close approach of hydrogen atoms combined with 2-C atoms to proton acceptors located on the surface, resulting in the high preference for Δ2-olefin production. On the contrary, the MOR zeolite used as a reference catalyst induces poor selectivity due to the close packing of epiandrosterone in its linear micropores. The very small tolerance in the space between epiandrosterone and the pore wall causes similar probabilities to hydrogen atoms combined to 2-C and 4-C atoms reacting with the proton acceptors located on the surface, thereby inducing similar selectivity for both Δ2- and Δ3-olefins.

Large port zeolites with pore entrances composed of 12 membered oxygen atoms (12 MR) allow the transfer of epiandrosterone into their micropores, but the diffusion rate and adsorption state of epiandrosterone in their micropores differ according to their pore structures. MOR zeolite has one-dimensional, linear pores (0.7 nm × 0.65 nm), BEA zeolite has three-dimensionally connected, sinusoidal pores (0.76 nm × 0.64 nm), FAU zeolite has supercages connected through 12 MR pore entrances (7.4 Å), and LTL zeolite also has 12 MR linear pores (7.1 Å) with periodically repeated large void spaces (aperture of 12.6 Å). Since their pore shapes and sizes influence the diffusion and conformation of epiandrosterone in their pores, the conversion of epiandrosterone and the selectivity for Δ2-olefin over these zeolites are strongly dependent on their pore structures.

Our previous work on the mesoporous materials incorporated with sulfonic acid groups were not suitable for the investigation of the steric effect of catalysts. In this study, we used five kinds of zeolite with different pore sizes and shapes as catalysts to investigate the effect of zeolite pore structure on their catalystic activity and selectivity in the dehydration of epiandrosterone. Although MFI zeolite has 10 MR pore entrances (5.3 Å), which are too small to allow the diffusion of epiandrosterone, it was used to verify the contribution of the external surface to its activity by silane masking. The conversion and selectivity for Δ2-olefin in the dehydration were measured over the zeolites. Their epiandrosterone uptake was also examined in order to investigate the diffusion rate of epiandrosterone in zeolite pores. In addition, the conformation of epiandrosterone in zeolite micropores was simulated by theoretical calculations to reveal clearly the limitation exerted by pore structure on the adsorption of large molecules. The variation of the conversion and selectivity in the dehydration over the zeolites is discussed relating to their pore structure and acidity.

2. Experimental

2.1. Preparation of catalysts

Five kinds of zeolite BEA, FAU, LTL, MOR and MFI, were used as catalysts in the dehydration of epiandrosterone. The Si/Al molar ratios of the zeolites were varied in order to investigate the effect of acidity on the conversion and selectivity in the dehydration. Their Si/Al ratios and sources are listed in Table 1. All H-form zeolites used, except LTL zeolite, were commercial products. The numbers in their names after the framework codes represent their Si/Al ratios.

LTL zeolite was hydrothermally synthesized following the procedure described in the literature [18]. A synthetic mixture of LTL zeolite was prepared using sodium aluminate ($NaAlO_2$, 31% Na_2O, 34% Al_2O_3, Kanto), potassium hydroxide (93%, Daejung), sodium hydroxide (98%, Daejung) and colloidal silica (Ludox, 40% SiO_2, Aldrich). The composition of the mixture was 5.4 K_2O:5.7 Na_2O:1 Al_2O_3:30 SiO_2:500 H_2O. After aging for 24 h at ambient temperature, the mixture was hydrothermally reacted in an autoclave

Table 1
List of sources and properties of zeolites used in the study.

Catalyst	Pore diameter (Å)	Si/Al molar ratio	S_{BET} (m^2/g)	Amount of ammonia desorbed (mmol/g)	Source
MFI(25)	5.1 × 5.5,	25	425	0.26	Zeolyst Co.
MFI(75)	5.3 × 5.6	75	410	0.11	PQ Corp.
MOR(10)	6.5 × 7.0,	10	400	0.59	Tosoh Corp.
MOR(100)	2.6 × 5.7	100	420	0.10	Tosoh Corp.
BEA(13)	6.6 × 6.7,	13	880	0.38	PQ Corp.
BEA(100)	5.6 × 5.6	100	550	0.10	Seneca Co.
LTL(15)	7.1 × 7.1	15	280	1.18	Synthesized
FAU(2.6)	7.4 × 7.4	2.6	550	1.08	JRC-22[a]
FAU(6.7)		6.7	600	0.13	Tosoh Corp.
FAU(15)		15	780	0.26	Zeolyst Co.
FAU(30)		30	720	0.18	Zeolyst Co.
FAU(40)		40	780	0.08	Zeolyst Co.
FAU(180)		180	650	0.00	Zeolyst Co.
H_2SO_4/SiO_2	–	–	200	–	Prepared

[a] Japanese reference catalyst.

under autogenous pressure at 170 °C for 24 h. Zeolite cake obtained through washing and filtering was calcined at 550 °C for 8 h. H-form LTL zeolite was obtained by calcining ammonium ion-exchanged LTL zeolite using 0.25N ammonium nitrate at 550 °C for 8 h.

BEA(100), FAU(6.7) and MOR(100) zeolites were treated with dimethyl dichlorosilane (DMS, Aldrich) and *t*-butyl chlorodiphenyl silane (DPS, Aldrich) to mask the zeolite acid sites. The molecular diameters of DMS, and DPS, determined using ChemDraw were 4.5 Å × 2.0 Å and 9.1 Å × 6.5 Å, respectively, indicating that DMS but not DPS can diffuse into the micropores of the large port zeolites. Two grams of each zeolite sample was added to 100 ml anhydrous acetone (99.5%, Daejung) and stirred for 30 min to remove the water [19]. After filtering the zeolite slurry, the filtered zeolite was suspended in 50 ml *n*-hexadecane (99%, Aldrich). One gram of DPS was added dropwise to the slurry followed by heating at 150 °C. The mixture was cooled to 50–60 °C and washed with a mixture of *n*-hexane (95%, Aldrich) and dichloromethane (99.8%, Aldrich). DPS-treated zeolites [DPS-MFI(75), etc.] were obtained by drying in vacuum. For the DMS treatment, the zeolite samples were exposed to DMS vapor in a closed jacket chamber at 70–80 °C for 1 h. After DMS vapor was evacuated, the DMS-treated zeolites were dried at 70–80 °C [DMS-MOR(100), etc.].

A sulfuric acid catalyst impregnated on silica was also prepared. Water contained in the silica gel (0.063–0.2 mm, Merck) was continuously removed using a Dean-Stack apparatus by refluxing its slurry suspended in toluene (99.5%, Daejung). After removing the water, toluene was replaced with methanol (99.8%, Aldrich). At ambient temperature, sulfuric acid (95%, Aldrich) was added to the silica slurry up to 3 wt%. The sulfuric acid catalyst, H_2SO_4/SiO_2, was obtained by evaporating methanol and was stored by sealing to prevent water contamination.

2.2. Characterization of the catalysts

2.2.1. X-ray diffraction (XRD)

XRD patterns of the catalysts were recorded on an X-ray diffractometer (D/MAX-1200, Rigaku) at 40 kV and 40 mV.

2.2.2. Nitrogen adsorption

Adsorption isotherms of nitrogen were obtained using a volumetric adsorption measuring apparatus (Mirae SI nanoPorosity-XG). A zeolite sample of 0.1 g was charged in a sample tube and evacuated at 250 °C for 2 h. The surface areas of the zeolites were calculated by applying the Brunauer–Emmett–Teller (BET) equation from the nitrogen adsorption isotherms measured at 77 K.

2.2.3. Temperature-programmed-desorption (TPD) of ammonia

The TPD profiles of ammonia from the zeolites were recorded on a homemade TPD apparatus. A zeolite sample (0.1 g) charged in a quartz tube with an outer diameter of 9.5 mm was activated in a helium flow of 100 ml/min at 550 °C for 1 h. The zeolite sample was saturated with pulses of ammonia (99.999%, Korea gas) followed by purging with helium flow at 150 °C for 1 h. The TPD profiles were recorded as the sample temperatures were increased to 800 °C at a rate of 10 °C/min. Desorbed ammonia was monitored by a mass spectrometer (Balzers, QMS 200).

2.3. Dehydration of epiandrosterone

Epiandrosterone was dehydrated over the zeolites following the procedure described in our previous paper [17]. Epiandrosterone was purchased from Tokyo Kasei Inc. Two grams of epiandrosterone (6.9 mmol) was dissolved in toluene (99.5%, Daejung) and reacted over a 2 g of catalyst in a three-neck flask. Water produced during the dehydration was continuously removed by a Dean-Stack apparatus. Products were analyzed an HPLC (Agilent 1200) with an Inertsil ODS3 150 mm × 4.6 mm column. The conversion of epiandrosterone was defined as the mole percent of its consumption. The selectivity for Δ2-olefin was defined as the mole percent of Δ2-olefin produced per epiandrosterone consumed.

2.4. Uptake of epiandrosterone

Equal amounts (250 mg) of epiandrosterone and an internal standard (1S,2S,4R)-1-methyl-2-(phenyl-thio)-4-(prop-1-en-2-yl) cyclohexanol (MPTPH), were dissolved in 50 ml of methylene chloride. Since the kinetic diameter of MPTPH estimated using ChemDraw was 0.9 nm and its diameter was clearly larger than the pore entrances of the zeolites used in this study, MPTPH could not be adsorbed into zeolite pores.

After adding 1.0 g of zeolite to 10 ml of the epiandrosterone solution, the slurry containing zeolite was stirred by a magnetic stirrer in a constant water bath of 25 °C. Samples collected at a preset interval were filtered with a microfilter and dried with nitrogen flow followed by dilution with 1.5 ml CDCl3 (Aldrich). NMR spectra were recorded on an NMR spectrometer (Varian 300) and the uptake of epiandrosterone on zeolite was calculated from the change in the ratio of the peak at 3.6 ppm to the peak at 4.75 ppm. The former was attributed to the proton of the 3-C atom of epiandrosterone, while the latter to the protons of methylene of MPTPH. The internal standard method showed a good

reproducibility in determining the uptake of epiandrosterone on the zeolites.

2.5. Theoretical calculation

The unit cell structures of FAU, MOR and BEA zeolites were constructed based on the results of X-ray crystallographic study [20]. They were three-dimensionally expanded to $1 \times 1 \times 1$, $1 \times 1 \times 4$ and $2 \times 2 \times 1$ to build models of dehydrated H-form zeolites of FAU(6.7) ($H_{25}Si_{167}Al_{25}O_{384}$), MOR(95) ($H_2Si_{190}Al_2O_{384}$) and BEA(122) ($H_2Si_{244}Al_2O_{512}$), respectively. Aluminum atoms were randomly distributed on the tetrahedral sites composing the framework of each model obeyed the Loewenstein's rule. Extraframework protons, which compensated for the negative charges of the framework, were initially positioned around the aluminum atoms.

The charge equilibration method using QEq-charged1.1 was applied to determine the net atomic charges of hydrogen, silicon, aluminum and oxygen atoms [21]. After constructing the model structures, we selected energy-minimized structures based on their energy calculated using the conjugate gradient algorithm and the Buchart1.02-Universal1.01 force field [22,23]. The parameters relating to the interaction between the framework and the adsorbed epiandrosterone were derived from both force fields by the geometric combination rule.

In order to determine the conformation of epiandrosterone in the zeolite pores, we used Monte Carlo simulation. The structures of the host zeolites were assumed to be rigid during the epiandrosterone adsorption. Although some redistribution of protons can occur during adsorption, the migration of protons was not considered. Only one epiandrosterone molecule moved inside the zeolite pores to maximize their stabilization energy. The periodic boundary conditions were applied in all three dimensions during simulation and the Metropolis scheme was used. The average conformations of epiandrosterone were obtained from the calculation results after 3×10^6 iterations. The cutoff distance for a short-range Lennard–Jones summation was 15 Å and that for Ewald summation was the half of the unit cell length.

Since the zeolite frameworks were assumed to be rigid, only the non-bond interaction energy between the framework and epiandrosterone was calculated to obtain its optimized conformation in the pores of the FAU(6.7), MOR(95) and BEA(122) zeolites. The total interaction energy was the sum of the long-range Coulombic term and the short-range van der Waals (vdW) term. The vdW interaction parameters, D_0 and σ_0, are summarized in Table 2. After carrying out the adsorption simulation of epiandrosterone, the energies of the whole zeolite structures containing epiandrosterone molecules were minimized again to obtain more reliable conformations of epiandrosterone in the zeolite pores. Green lines were employed to denote the interaction between the protons of zeolites and the oxygen atoms of epiandrosterone.

Table 2
Lennard–Jones potential energy parameters used for the adsorption simulation[a].

Atom type	D_0 (kcal/mol)	σ_0 (Å)
Si_z[b]	0.0469	4.2000
Al_z[b]	0.0292	4.2400
O_z[b]	0.1648	3.3000
H	0.0440	2.8860
C	0.1050	3.8510
O	0.0600	3.5000

[a] The Buchart1.02-Universal1.01 force field which was developed to describe the energetics of zeolites–organic molecule systems was employed. The Burchart force field treated the zeolite framework and the Universal force field treated the intra- and intermolecular interactions. The parameters for the framework–molecule interactions are derived from parameters from both force fields, combining through the geometric combination rule.

[b] Si_z, Al_z and O_z represented silicon, aluminum and oxygen atoms in the zeolite framework, respectively.

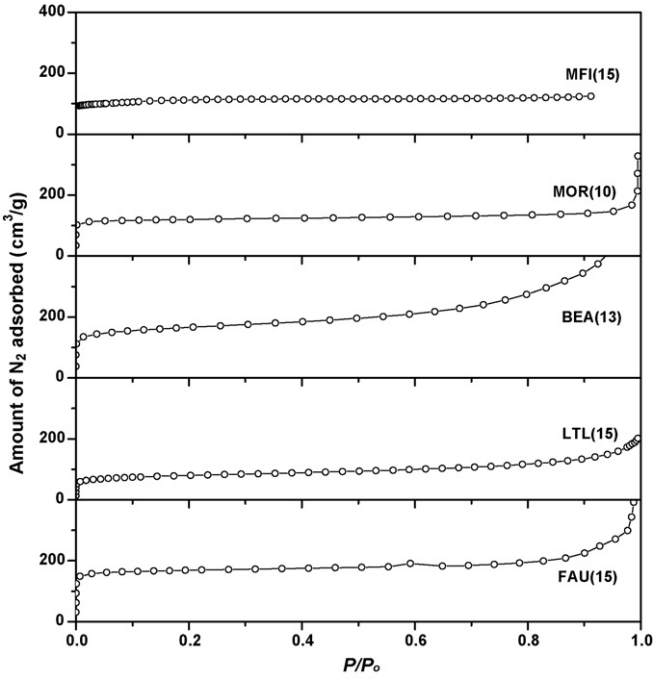

Fig. 1. N_2 adsorption isotherms of representative zeolites.

3. Results and discussion

Micropores of the zeolites caused Langmuir-type adsorption isotherms of nitrogen, as shown in Fig. 1. The slight increase in the nitrogen adsorption on BEA(13) zeolite at higher P/P_0 was attributed to its small particles composed of mesopores in its aggregates [24]. BEA(13) and FAU(15) zeolites had slightly large amounts of nitrogen adsorption because of their larger void volumes. MFI(25) and MOR(10) zeolites commonly showed similar intersections at $P/P_0 = 0$, about 100 cm^3/g, indicating their similar surface areas. The low intersection on LTL(15) zeolite caused its small surface area.

The TPD profiles of ammonia from the zeolites varied considerably with their topologies and Si/Al molar ratios, as shown in Fig. 2. The temperature of a desorption peak maximum (T_m) corresponded to the acid strength and the peak area to the number of acid sites. The T_m of MOR(10) zeolite was about 500 °C, indicating its highest acid strength among the tested zeolites, whereas BEA(13) zeolite exhibited a T_m of 280 °C due to its weak acidity. MFI(25) and LTL(15) zeolites had acid sites with medium strength. FAU zeolites with different Si/Al molar ratios presented different areas of desorption peaks, while the temperatures at the maxima of their desorption peaks were almost the same. To summarize these results, the acid strength of the zeolites increased in the following order: BEA < LTL ≈ FAU = MFI < MOR. The number of acid sites was strongly dependent on their Si/Al molar ratio.

The Si/Al molar ratios, BET surface areas and desorbed amounts of ammonia of the zeolites used in this study are listed in Table 1. The increased Si/Al molar ratio of the zeolites decreased the amount of ammonia desorbed, whereas this relationship was not quantitatively valid throughout all the zeolites with different topologies. FAU(6.7) zeolite had an unexpectedly small number of acid sites, despite its high aluminum content. This difference was attributed to the presence of extraframework aluminum that was not involved in the formation of acid sites [25]. Although all the zeolites except

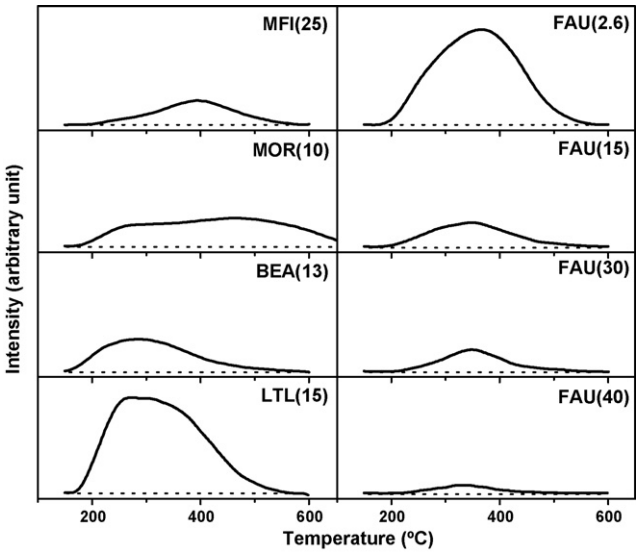

Fig. 2. TPD profiles of ammonia from representative zeolites. TPD profiles from four kinds of FAU zeolites are also shown to exhibit the effect of their Si/Al molar ratio on the number of acid sites.

LTL(15) had large BET surface areas above 400 m^2/g, BEA and FAU zeolites showed large BET surface areas of approximately 800 m^2/g as expected from their nitrogen adsorption isotherms.

Due to its molecular diameter of about 5 Å, epiandrosterone can enter into the pores of 12 MR zeolites and can be dehydrated over their acid sites. Fig. 3 shows the dehydration over MOR(100), BEA(100) and FAU(6.7) zeolites. A supported acid, H_2SO_4/SiO_2 was also used to reveal the effect of pore structure on the dehydration. H_2SO_4/SiO_2 and BEA(100) zeolite showed high conversion, while the conversion on MOR(100) zeolite was very low. FAU(6.7) zeolite had a slightly low conversion compared to BEA(100) zeolite. The selectivity for Δ2-olefin varied according to the catalysts. FAU(6.7) zeolite maintained a high selectivity around 95% throughout the dehydration reaction, while BEA(100) and MOR(100) zeolites showed low selectivities of about 60%. The supported catalyst with macropores exhibited medium selectivity, with very high conversion on it. The high conversions over H_2SO_4/SiO_2 and BEA(100) zeolite simply demonstrated the dependence of the conversion on the diffusion rate of epiandrosterone. MOR(100) zeolite with the strongest acidity showed the lowest conversion among these catalysts. Therefore, the large difference in the conversion of BEA(100) zeolite from MOR(100) zeolite indicated the absence of any coincident relationship between the conversion and acidity of these zeolites.

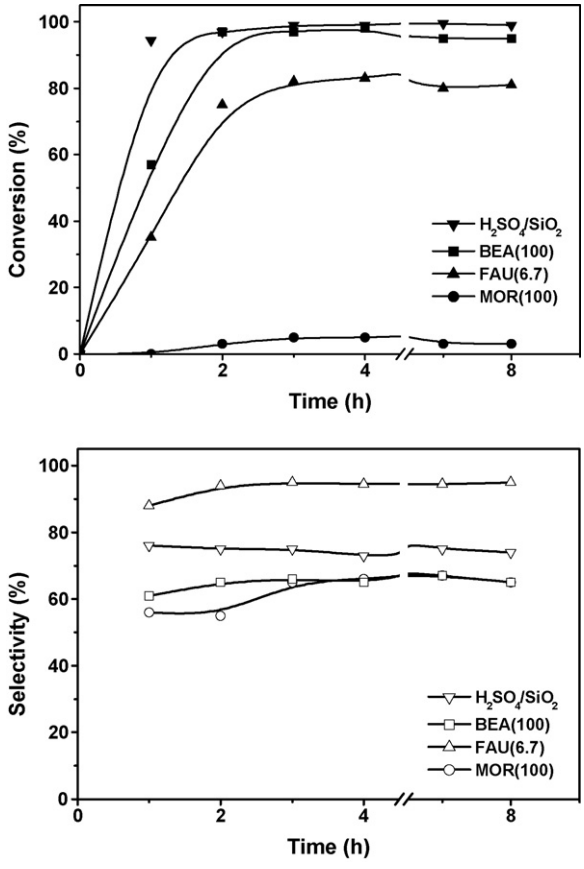

Fig. 3. Dehydration of epiandrosterone over representative zeolites at 110 °C (epiandrosterone/catalyst = 0.5 g/0.5 g, solvent; toluene).

The catalytic contribution of the external or internal surface of zeolites can be elucidated by changing their particle size as reported in many literatures [5,6,26,27]. However, it was very difficult obtain several kinds of zeolites with similar particle sizes and particle shapes. Therefore, we employed the silination on the zeolites using two kinds of silanes with considerably different molecular sizes (DPS and DMS) to compare the effect of the external surface on their catalytic activity. The modification of zeolites with DPS and DMS silanes is helpful to confirm the progress of the dehydration in their micropores. Table 3 lists the catalytic performance of silane-modified zeolites. Since the conversion of epiandrosterone and the selectivity for Δ2-olefin over the zeolites approached equilibrium after 3 h, as shown in Fig. 3, the conversion and selectivity obtained at 3 h were used to compare their catalytic performance. The reaction time was shortened to 2 h on BEA zeolites due to the very rapid reaction over them.

The DMS-modified MOR(100) and BEA(100) zeolites, regardless of their topology, showed negligible conversions, indicating that the small molecular size of the DMS allowed it to mask completely their acid sites, even in the micropores. However, DPS-modified BEA(100) and FAU(6.7) zeolites maintained their catalytic activity, indicating that the acid sites located in the micropores of DPS-BEA(100) and DPS-FAU(6.7) zeolites were still active, because DPS only masks the acid sites located on the external surface. Even though the masking of acid sites located on the external surface caused the decrease in the total number of acid sites, the conversion over FAU(6.7) increased with the silination by DPS. The silination on the external surface of MOR zeolites with low Si/Al molar ratios suppresses the carbon deposit on it and prevents the blocking of pore mouth, resulting in the increase of the conversion in the liquid-phase degradation of polyethylene [28]. The silination might increase the activity of the FAU(6.7) catalyst by suppressing the carbon deposit on their external surface and extend its catalyst life.

Table 3
Dehydration of epiandrosterone over silane-modified zeolites.

Catalyst	Conversion (%)	Selectivity (%)
MFI(75)	28	74
DPS-MFI(75)	05	–
MOR(100)	10	65
DMS-MOR(100)	00	–
DPS-MOR(100)	05	–
BEA(100)	99	70
DMS-BEA(100)	05	–
DPS-BEA(100)	85	75
FAU(6.7)	80	95
DPS-FAU(6.7)	91	96

Reaction condition: Epiandrosterone/catalyst = 0.5 g/0.5 g, solvent; toluene. Reaction was carried out for 3 h, but for 2 h over BEA(100).

Table 4
Dehydration of epiandrosterone over zeolites with different Si/Al molar ratios.

Catalyst	Conversion (%)	Selectivity (%)
MFI(25)	31	78
MFI(75)	28	74
MOR(10)	3.5	60
MOR(100)	10	65
BEA(13)	92	65
BEA(100)	99	70
LTL(15)	0	0
FAU(2.6)	21	95
FAU(6.7)	80	95
FAU(15)	81	93
FAU(30)	77	92
FAU(40)	37	95
FAU(180)	5	95

Reaction condition: Epiandrosterone/catalyst = 0.5 g/0.5 g, solvent; toluene. Reaction was carried out for 3 h, but 2 h over BEA(13) and BEA(100).

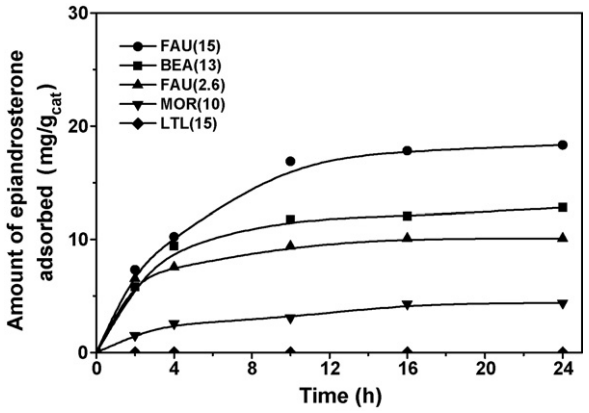

Fig. 4. Uptake of epiandrosterone on representative zeolites at 25 °C.

Since MOR(100) zeolite itself showed poor catalytic activity, the low conversion on DPS-MOR(100) zeolite was not due to the DPS modification. The reduction of the conversion on MFI(75) zeolite induced by the DPS modification indicated that the acid sites located on its external surface also participated in the dehydration, because its 10 MR-sized micropores did not allow the diffusion of epiandrosterone into its micropres. Therefore, the very low conversion on DMS-BEA(100) zeolite and the retained high conversion on DPS-BEA(100) zeolite strongly indicated that the dehydration of epiandrosterone mainly occurred in the 12 MR-sized micropores of BEA zeolite

Table 4 lists the conversion and selectivity obtained over all the zeolites used in this study. The conversions over the zeolites differed considerably according to their topology. MFI and MOR zeolites showed low conversions, while BEA zeolites showed high conversions of about 90%, even at 2 h. No dehydration occurred over LTL(15) zeolite, whereas the conversion over FAU zeolites varied widely according to their Si/Al molar ratio. The selectivity for Δ2-olefin over the zeolites also varied according to their topologies. MFI, MOR and BEA zeolites showed a medium selectivity of about 60–70%, regardless of the conversion level over them, whereas the selectivities over FAU zeolites were consistently above 90%, although the conversion over them varied from 5 to 80%.

These results suggested that the pore structure and acidity of the zeolites combined to determine the conversion and selectivity in the dehydration. The low conversion over FAU(40) and FAU(180) zeolites with high Si/Al molar ratio was responsible for the low acid site concentration. However, the high conversions over BEA(13) and BEA(100) zeolites emphasized the effect of the pore structure, because BEA(100) zeolite only had few weak acid sites. MOR(10) zeolite with numerous strong acid sites and LTL(15) zeolite with numerous weak acid sites commonly showed very low conversion, strongly suggesting the importance of pore structure in determining the conversion in the dehydration. The conversion was primarily dependent on the pore structure of the zeolites, and the strong acid sites were not essential for the dehydration.

In order to verify the effect of pore structure on the dehydration reaction over the zeolites, the epiandrosterone uptake on them was examined (Fig. 4). The uptake rates of epiandrosterone on the zeolites varied considerably according to their pore structures, although their pore entrances were commonly composed of 12 MR. The zeolites with FAU and BEA topologies showed rapid diffusion of epiandrosterone into their pores, resulting in high uptake rates, whereas the uptake rate on MOR(10) zeolite was very slow. The excessively small uptake amount on LTL(15) zeolite suggested the prohibited diffusion of epiandrosterone into its pores. Thus, a zeolite pore structure that allows the rapid diffusion of epiandrosterone is indispensable for its high conversion.

The consistently high selectivity for Δ2-olefin over FAU zeolites, regardless of their Si/Al molar ratio, also indicated the importance of pore structure on the selectivity in the dehydration. The tilted orientation of epiandrosterone on the sulfonic acid sites incorporated on the MCM-41 mesoporous material caused a high selectivity due to the suppressed the close approach of the hydrogen atom com-

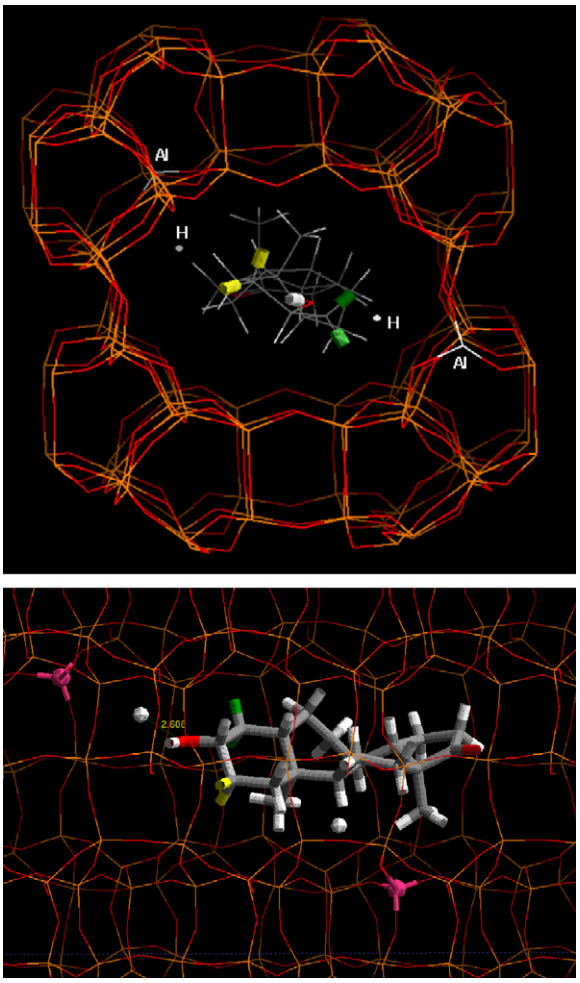

Fig. 5. Simulated conformation of epiandrosterone in MOR(95) zeolite. The hydrogen atoms of epiandrosterone that can produce Δ2-olefin and Δ3-olefin are represented by the yellow and green colors of cylinder forms, respectively. The hydrogen atom of hydroxyl group is represented by the white color of cylinder form. (For interpretation of the references to color in this figure legend, the reader is referred to the web version of the article.)

bined to the 2-C atom to the proton acceptors located on the surface [17]. Therefore, the preferable adsorption states of epiandrosterone in the micropores of the zeolites determined the selectivity for Δ2-olefin.

The simulated adsorption states of epiandrosterone on MOR(95), BEA(122) and FAU(6.7) zeolites differed considerably according to their pore structure, as shown in Figs. 5–7. A linear epiandrosterone molecule was closely packed in the linear pore of MOR(95) zeolites (Fig. 5). Since the molecules preferred the paralleled conformation to the linear pore, they exhibited no preference for the selective dehydration. The low probability for the approach of hydroxyl groups of epiandrosterone molecules to the surface protons may have been responsible for the very low conversion on MOR(95) zeolite.

Even though the micropores of BEA zeolite were composed of 12 MR, as were those of MOR zeolites, the intersected spaces of the pores of the former were much larger than those of the latter. As shown in Fig. 6, the epiandrosterone molecules had margins in the pores of BEA zeolite. The close approach of the hydroxyl group to the proton on the surface was also allowed. However, the distance between the molecule and the pore wall remained insufficient to conform for the tilted adsorption of epiandrosterone to reduce the steric hindrance induced by the adsorption of it. On the contrary, the supercages of FAU zeolite provided sufficient space for the adsorption of epiandrosterone by tilting-induced minimization of steric hindrance, as shown in Fig. 7. An epiandrosterone molecule can be adsorbed with the preferred orientation, thereby minimizing the steric hindrance.

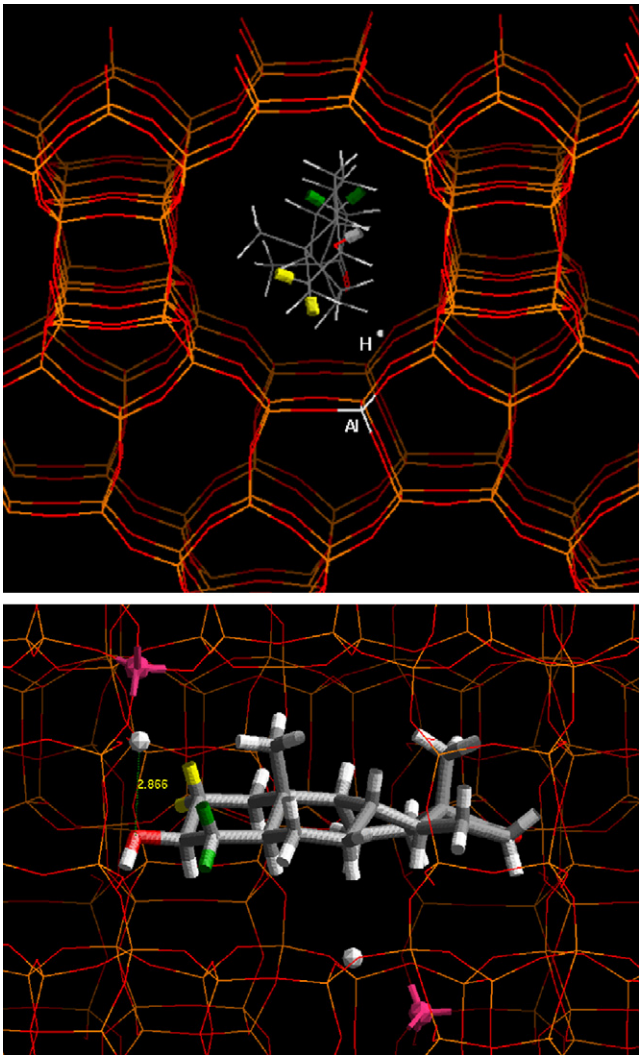

Fig. 6. Simulated conformation of epiandrosterone in BEA(122) zeolite. Details of drawing were the same in Fig. 5.

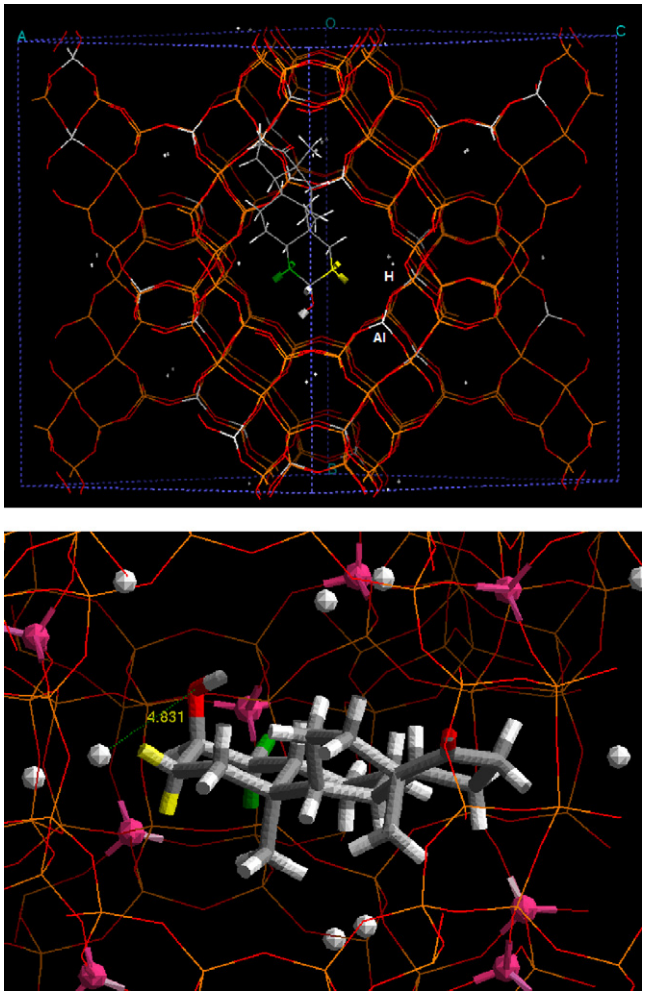

Fig. 7. Simulated conformation of epiandrosterone in FAU(6.7) zeolite. Details of drawing were the same in Fig. 5.

The close packing of epiandrosterone in MOR zeolite resulted in low conversion and poor selectivity for Δ2-olefin because of the slow diffusion and low probability for the specific orientation with small steric hindrance. The sinusoidal and three-dimensionally interconnected pores of BEA zeolite allowed the rapid diffusion of the epiandrosterone molecules, but their conformation in the pores was not free due to the small margins between the molecule and the wall. However, the supercages of FAU zeolite were very large for an epiandrosterone molecule, thus permitting its various orientations. The sufficient supercage space allowed the adsorption of epiandrosterone with tilted conformation that had the lowest steric hindrance, thus achieving an exceptional selectivity for Δ2-olefin.

4. Conclusions

The masking of acid sites located on the external surface of the zeolites and the epiandrosterone uptake on them confirmed the dehydration of epiandrosterone in 12 MR micropores of MOR, BEA and FAU zeolites. Since the conversion of epiandrosterone was primarily limited by its diffusion rate, the zeolite pore structures were very important in determining the conversion of the dehydration. In addition, the zeolite pore structures also affected the selectivity for

Δ2-olefin in the dehydration, because they limited the conformation of epiandrosterone in micropores. The number of acid sites of the zeolites, as deduced from their Si/Al molar ratio, became important to determine the conversion when the mass transfer limitation was not severe. The close packing of the epiandrosterone molecule in MOR zeolite caused an extremely low conversion with poor selectivity due to both the extremely slow diffusion in the pores and the absence of any choice in the adsorption conformation. On the contrary, FAU zeolite with large supercages provided enough space for the epiandrosterone molecule to minimize the steric hindrance by tilting its end part, thereby affording high selectivity for Δ2-olefin.

Acknowledgement

This work was supported by the Korea Research Foundation Grant (MOEHRD) (KRF-2007-412-J02001).

References

[1] K. Yoo, E.C. Burckle, P.G. Simirniotis, J. Catal. 211 (2002) 6–18.
[2] F. Houot, L. Grasset, P. Magnoux, A. Ambles, J. Mol. Catal. A: Chem. 265 (2007) 117–126.
[3] V.J. Rao, S.R. Uppili, D.R. Corbin, S. Schwarz, S.R. Lustig, V. Ramamurthy, J. Am. Chem. Soc. 120 (1998) 2480–2481.
[4] M. de Bruyn, S. Coman, R. Bota, V.I. Parvulescu, D.E. de Vos, P.A. Jacobs, Angew. Chem. 115 (2003) 5491–5494.
[5] C. Tsangarakis, C. Raptis, E. Arkoudis, M. Stratakis, Adv. Synth. Catal. 350 (2008) 1587–2908.
[6] C. Tsangarakis, I.N. Lykakis, M. Stratakis, J. Org. Chem. 73 (2008) 2905–2908.
[7] M. Jennifer, M.B. Hunter, New Engl. J. Med. 332 (1995) 1691.
[8] A. Kleemann, J. Engel, Pharmaceutical Substance: Synthesis, Patents, Application, fourth ed., Thime, 2000, pp. 1152, 1647, 1829, 2160.
[9] M.I. Merlani, L.S. Amiranashvili, E.P. Kemertelidze, K. Papadopulos, E. Yannakopulu, Chem. Nat. Compd. 42 (2006) 313–315.
[10] M.I. Merlani, M.G. Davitishvili, N.S. Nadaraia, M.I. Sikharulidze, K. Papadopulos, Chem. Nat. Compd. 40 (2004) 144–146.
[11] R.E. Counsell, P.D. Klimstra, USP 3,098,851 (1963).
[12] T. Iida, T. Momose, F.C. Chang, J. Goto, T. Nambara, Chem. Pharm. Bull. 37 (1989) 3323–3329.
[13] P. Crabbe, C. Leon, J. Org. Chem. 35 (1970) 2594–2596.
[14] T. Nishiguchi, N. Machida, E. Yamamoto, Tetrahedron Lett. 28 (1987) 4565–4568.
[15] F. D'Onofrio, A. Scettri, Synthesis (1985) 1159–1161.
[16] F. Chavez, S. Suerez, M. Diaz, Synth. Commun. 24 (1994) 2325–2339.
[17] O.Z. Kwon, J.W. Park, S. Kang, J.Y. Lee, G. Seo, Catal. Commun. 9 (2008) 2312–2315.
[18] G. Artioli, A. Kvick, Eur. J. Miner. 2 (1990) 749–759.
[19] W.S. Ahn, D.H. Lee, T.J. Kim, J.-H. Kim, G. Seo, R. yoo, Appl. Catal. A: Gen. 181 (1999) 39–49.
[20] http://topaz.ethz.ch/IZA-SC/StdAtlas.htm.
[21] Cerius2, Simulation package of version 4.10 developed by Accelrys Inc.
[22] E.V. de Burchart, Ph.D. Thesis, Studies on zeolites: molecular mechanics, framework stability and crystal growth, Table I, Chapter XII, 1992.
[23] A.K. Rappe, C.J. Casewit, K.S. Colwell, W.A. Goddard III, W.M. Skiff, J. Am. Chem. Soc. 114 (1992) 10024–10035.
[24] M.A. Camblor, A. Corma, S. Valencia, Micropor. Mesopor. Mater. 25 (1998) 59–74.
[25] B. Xu, S. Bordiga, R. Prins, J.A. van Bokhoven, Appl. Catal. A: Gen. 333 (2007) 245–253.
[26] A. Banito, A. Corma, H. García, J. Primo, Appl. Catal. A: Gen. 116 (1994) 127–135.
[27] M.J. Clement, A. Corma, H. García, J. Primo, Appl. Catal. 51 (1989) 113–125.
[28] S.W. Jeong, Y.S. You, J.H. Kim, G. Seo, Stud. Surf. Sci. Catal. 145 (2003) 469–470.